

# Enhanced Fault Diagnosis Using Broad Learning for Traction Systems in High-Speed Trains

Chao Cheng , Member, IEEE, Weijun Wang , Hongtian Chen , Member, IEEE, Bangcheng Zhang , Junjie Shao , and Wanxiu Teng

**Abstract**—Faults happen inevitably in traction systems and thus place the security of the whole high-speed train at risk. In order to improve the safety and reliability of high-speed trains, this article deals with fault detection and diagnosis (FDD) problem for traction systems. Because of high sampling frequency of equipped sensors, FDD strategies in the supervision system of high-speed trains should be of enough high computation efficiency, which is a great bottleneck for artificial intelligence-based FDD methods. For reducing the computational load while maintaining the satisfactory diagnostic accuracy, an enhanced FDD architecture using the modified principal component analysis and broad learning system is developed in this article. Based on the proposed data-driven design whose core is to extract fault information, fast and accurate FDD can be achieved without requirements for mathematical models or control mechanism of high-speed trains. The effectiveness and feasibility of the proposed online design are illustrated on the traction control platform of high-speed trains.

**Index Terms**—Broad learning system (BLS), fault detection and diagnosis (FDD), high-speed trains, principal component analysis (PCA), traction systems.

## I. INTRODUCTION

MODERN high-speed trains have been witnessing a rapid development in the past two decades [1]–[8]. However, the associated railway accidents have happened unexpectedly over the world [9]–[11]. As pointed out in [12], there are more than average seven serious accidents in a year. These catastrophes, which usually appeared in the form of explosions or fires,

Manuscript received August 5, 2020; revised October 19, 2020; accepted November 27, 2020. Date of publication December 10, 2020; date of current version March 5, 2021. This work was supported in part by the National Natural Science Foundation of China under Grant 61903047 and in part by the Jilin Science and Technology Department under Grant 20200401127GX. Recommended for publication by Associate Editor xx. (Corresponding author: Hongtian Chen.)

Chao Cheng and Weijun Wang are with the School of Computer Science and Engineering, Changchun University of Technology, Changchun 130012, China (e-mail: chengx415@163.com; jinwei312@163.com).

Hongtian Chen is with the Department of Chemical and Materials Engineering, University of Alberta, Edmonton, AB T6G 2V4, Canada (e-mail: chtbaylor@163.com).

Bangcheng Zhang is with the School of Mechatronic Engineering, Changchun University of Technology, Changchun 130012, China (e-mail: zhangbangcheng@ccut.edu.cn).

Junjie Shao is with the Data Research Office for CRRC Changchun Railway Vehicles Co., Ltd, Changchun 130062, China (e-mail: shaojunjie@cccr.com.cn).

Wanxiu Teng is with the National Engineering Laboratory, CRRC Changchun Railway Vehicles Co., Ltd, Changchun 130062, China (e-mail: tengwanxiu@cccr.com.cn).

Color versions of one or more figures in this article are available at <https://doi.org/10.1109/TPEL.2020.3043741>.

Digital Object Identifier 10.1109/TPEL.2020.3043741

conflicts, derailments, etc., were caused by faults or failures of high-speed trains. For instance, in Los Angeles of USA, a train collision happened in 2008. In addition, Because of the failure of signaling systems in a train, a devastating accident took lives of more than 40 people on the Yongwen Line in China. Therefore, the fundamental demands for improving reliability of high-speed trains should continue to draw increasing attention from transportation community [10]. Hence, early diagnosis of faults are of significant meanings before spectacular accidents happen [13].

Incipient faults, which will eventually evolve into large-magnitude faults or failures as time goes on, usually exist in high-speed trains [13]. Responsible reasons for these incipient faults include harsh operation environment [14], performance degradation of electrical units [15], [16], overloading condition [17], etc. Therefore, before incipient faults become large-magnitude faults or failures, their successful detection and diagnosis are essential for improving the reliability of traction systems.

It is well known that model-based fault detection and diagnosis (FDD) methods are powerful tools to deal with large-magnitude faults [10], [18], [19], which increase the reliable of systems [20], [21]. Indeed, their developments in the past one decade have built the mainstream in the field of transportation [22]–[25]. However, available or potential incipient FDD applications using methods based on models are rarely found in high-speed trains [26]. The main reason is that most of these method heavily depend on the mathematical models [27].

Another important branch of FDD applications for traction systems is the data-driven design whose main technological cores are multivariate statistical analysis (MSA) [17], [26], [28]–[31] and artificial intelligence (AI) techniques. Owing to their superior simplicity and scalability, data-driven design of FDD methods for high-speed trains has been extensively explored [10].

The first data-driven attempt using MSA is the multimode kernel principal component analysis (PCA) method proposed to detect incipient faults and common faults in IGBT of traction systems [17]. To accurately model systemic variations and uncertain noises in the traction system, deep PCA is first developed, based on which successful detection and isolation of incipient sensor faults are achieved [13]. Focusing on the non-Gaussian characteristic of signals measured from traction systems, the methods based on rotary principal and residual subspace are proposed, in which non-Gaussian signals can be transformed

into Gaussian ones [17]. In addition, the integration of randomized algorithms and canonical correlation analysis is proposed in [29] to find an optimal threshold for non-Gaussian signals measured from high-speed trains. In fact, there are different objective functions corresponding to MSA techniques to generate different projection rules for the FDD purpose. It should be emphatically noted that these obtained projections are the key steps in FDD applications, which is the so-called feature extraction. However, to the best of our knowledge, although MSA-based FDD methods can deal with high-frequency signals, only fault detection tasks could be achieved in high-speed trains.

A typical type of AI techniques is the artificial neural networks such as convolutional neural network (CNN), radial basis function neural network, extreme learning machine, etc. As summarized in [10], various FDD methods based on AI can be used to extract features with fault information from vibrations and audio signals. In [32], for example, the CNN is used to diagnose sensor faults in electric drive systems after fault detection. Whilst, multiple types of artificial neural networks, such as the radial basis function neural network, are employed as main tools for feature extraction in [33] to diagnose sensor faults in traction systems. The salient advantage of AI used for FDD is the nonlinear learning ability because it may provide more complex and complete results for feature extraction. However, time consuming is unavoidable, which produces some difficulties for online applications.

The recent advances about data-driven methods indicate promising potentials of FDD topics in traction systems. Nevertheless there are still some open problems. More specifically, the main challenges are as follows.

- 1) Only fault detection tasks can be achieved by FDD methods based on MSA.
- 2) The existing AI-based methods waste too much time in training and implementing.
- 3) Traction systems are characterized by high sampling frequency. It is not easy to design an online FDD scheme.

Strongly motivated by aforementioned discussions, an enhanced FDD method is urgently needed for the sake of reducing computational load while maintaining the satisfactory diagnostic performance in high-speed trains. In this article, a data-driven FDD method is proposed via the intensive integration of PCA and a broad learning system (BLS) where fast and accurate FDD implementation could be easily accomplished.

The rest of this article is organized as follows. In Section II, combining with an introduction of traction systems in high-speed trains and BLS, the purpose of this study is then formulated. In Section III, the proposed BLS-aided methodology for fast and accurate FDD is elaborated. In Section IV, multiple sets of experiments on the traction control platform of high-speed trains including FDD results and comparison analysis are conducted. Finally, conclusions are drawn in Section V.

## II. PRELIMINARIES

In this section, the traction systems and the BLS are firstly introduced, based on which the objective of this study is then formulated.

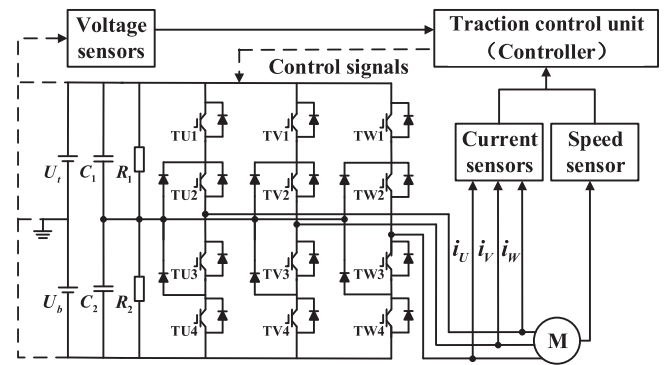


Fig. 1. Schematic diagram of traction systems in high-speed trains.

### A. Traction Systems of High-Speed Trains

In this article, the CRH2A-type high-speed train is taken into consideration in which four traction systems provide traction power of the entire train [4]. As presented in [8], the traction system is one core unit consisting of a traction control unit (TCU), a three-level source inverter (TSI), four induction motors, and filters, etc. Its control strategy is space vector pulsewidth modulation (SVPWM), and the corresponding schematic diagram is depicted in Fig. 1.

In the traction system of CRH2A-type high-speed trains, six sensors are equipped to collect real-time observations that will be used as the input of both the double proportional integral (PI) controller and the supervision unit. After setting a given traction speed, the TCU can achieve expected performance by adjusting gate control signals of TSI based on the SVPWM strategy. By comparing online samplings and the corresponding predesigned thresholds, the supervision unit adopted in existing high-speed trains maybe not effective for successful detection of parts' faults, and then an autoprotecting mode will be activated [8]. Actually, either high missing-alarm ratios (MARs) or high false alarm ratios (FARs) in traction systems of high-speed trains will lead to dissatisfactory FDD results and should be prohibitive. An acceptable tradeoff between the MAR and the FAR should be at least achieved for FDD tasks in traction systems.

### B. Broad Learning System

The BLS [34] is proposed based on the well-developed random vector functional-like neural network. It can achieve remarkable reduction of the computation loads by inheriting the network structure of random vector functional-like neural networks [35]. Generally, a BLS is flatted in the width instead of the deep structure by multiple enhancement nodes, and its basic neural network is depicted in Fig. 2. The core of BLS is to find the pseudoinverse of both feature and enhanced nodes to the target value, where these nodes correspond to the inputs of neural networks.

Based on the structure shown in Fig. 2, the formulation of BLS can be described as follows. For the input data  $X$ , the mapped feature can be first obtained by the following projection:

$$Z_i = \phi_i(XW_{e_i} + \beta_{e_i}^T), \quad i = 1, \dots, n \quad (1)$$

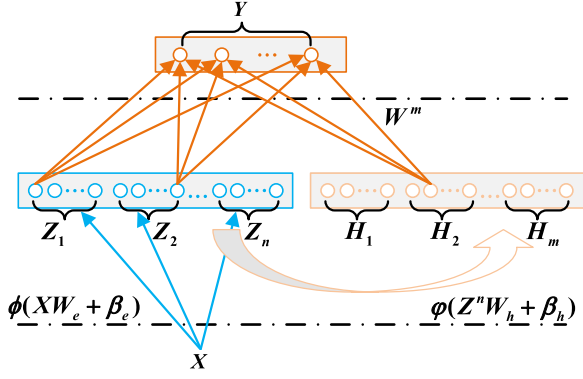


Fig. 2. Architecture of the broad learning system.

where  $\phi_i$  is the  $i$ th activation function,  $W_{e_i}$  and  $\beta_{e_i}$  are the  $i$ th random weight and random bias, respectively; they are generated from the correspondingly given probability density function. Assume that  $X$  is formed by  $N$  samplings with  $m$  variables and  $Z_i$  is of  $\kappa$  dimensions, then  $X \in R^{N \times m}$ ,  $W_{e_i} \in R^{m \times \kappa}$ ,  $\beta_{e_i} \in R^{\kappa \times N}$ , and  $Z_i \in R^{N \times \kappa}$ . Furthermore,  $Z^n$ , i.e., all the feature nodes of original dataset  $X$ , can be defined as

$$Z^n = [Z_1, Z_2, \dots, Z_n] \quad (2)$$

where  $Z^n \in R^{N \times \kappa n}$ . Then,  $m$  sets of enhancement nodes, as shown in Fig. 2, are obtained in the form of

$$H_j = \varphi_j(Z^n W_{h_j} + \beta_{h_j}^T), \quad j = 1, \dots, m. \quad (3)$$

Similar to (2), it is assumed that the dimension of the enhancement node is  $q$ , one has

$$H^m = [H_1, H_2, \dots, H_m] \quad (4)$$

where  $W_{h_j} \in R^{\kappa n \times q}$ ,  $\beta_{h_j} \in R^{q \times N}$ ,  $H_j \in R^{N \times q}$ , and  $H^m \in R^{N \times qm}$ . Finally, the output  $Y$  with  $c$  classes can be calculated as

$$Y = [Z^n | H^m] W^m \quad (5)$$

where  $Y \in R^{N \times c}$  and  $W^m \in R^{(kn+qm) \times c}$ . The essence of BLS is to find a proper  $W^m$ . Fortunately, BLS can provide a rapid solution (i.e., to obtain  $W^m$ ) compared with the existing deep learning methods. When the weights are obtained, the entire process is done.

### C. Objectives

As specially pointed out in [17], the univariate control charts are currently used in supervision subsystems of high-speed trains, which considers 41 types of faults. This method is effective only if serious component faults arise [16]. Obviously, this situation is unsatisfactory in practical FDD applications. Superadding the high sampling frequency of sensors in traction systems of high-speed trains, the objectives of this article designed for the FDD purpose are summarized as follows.

- 1) To characterize the traction systems of high-speed trains in a general framework without any assumptions.
- 2) To extract sufficient fault features used for incipient fault detection and diagnosis tasks.

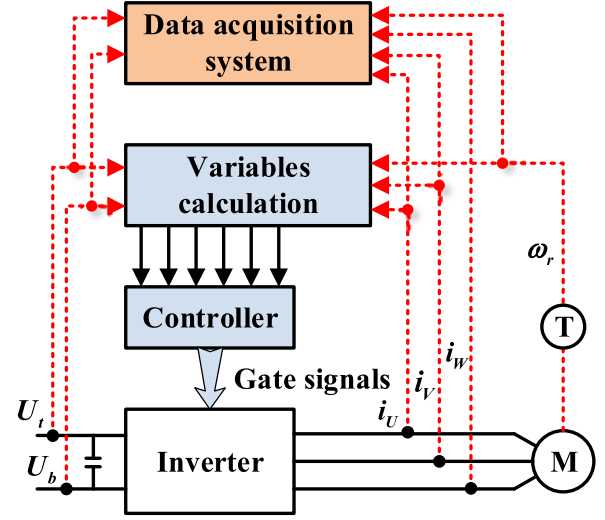


Fig. 3. Diagram of the traction system of high-speed trains.

- 3) To design a new FDD scheme with great computational efficiency for offline training and online implementation.

## III. PROPOSED METHODOLOGY USING BLS

In this section, collection and description of datasets are first presented, then the detailed fault diagnosis strategy using BLS method will be followed.

### A. Data Collection

As shown in Fig. 3, traction systems are placed with multiple sensors for specific purposes, such as process control and system monitoring [13].

In this article, stored in the data acquisition system in Fig. 3,  $K + 1$  terms of datasets are necessary to be used for model construction. Mathematically, these collected signals can be described in terms of

$$\underline{x} = [U_t \ U_b \ i_U \ i_V \ i_W \ \omega_r]^T \in R^6 \quad (6)$$

where  $U_t$  and  $U_b$  are voltages in two bridges,  $i_U, i_V$ , and  $i_W$  are three-phase input currents of traction motors, and  $\omega_r$  is the traction speed. Based on (6), consider  $K + 1$  operation conditions of the traction systems, the normal and fault datasets can be defined by

$$\begin{aligned} \underline{X}_{nr} &= [\underline{x}_{nr}(1) \ \dots \ \underline{x}_{nr}(N_{nr} + N_w)]^T \\ \underline{X}_{k,f} &= [\underline{x}_{k,f}(1) \ \dots \ \underline{x}_{k,f}(N_{k,f} + N_w)]^T \end{aligned} \quad (7)$$

where  $\underline{X}_{nr} \in R^{(N_{nr} + N_w) \times 6}$  and  $\underline{X}_{k,f} \in R^{(N_{k,f} + N_w) \times 6}$ ; the subscripts  $nr$  and  $f$  refer to the normal and fault conditions, respectively;  $N$  is the sampling number; and  $(k, f)$  denotes the  $k$ th fault type for  $k = 1, \dots, K$ .

### B. Fault Detection Using Mapped Features

To decrease the uncertainties hidden in (7), the moving average technique is introduced to preprocess  $\underline{X}_{nr}$  and  $\underline{X}_{k,f}$  as

follows:

$$\begin{aligned} X_{nr} &= [x_{nr}(1) \cdots x_{nr}(N_{nr})] \in R^{N_{nr} \times 6} \\ X_{k,f} &= [x_{k,f}(1) \cdots x_{k,f}(N_{k,f})] \in R^{N_{k,f} \times 6} \end{aligned} \quad (8)$$

where

$$\begin{aligned} x_{nr}(i) &= \frac{1}{N_w} \sum_{j=i}^{i+N_w} \underline{x}_{nr}(i), \quad i = 1, \dots, N_{nr} \\ x_{k,f}(i) &= \frac{1}{N_w} \sum_{j=i}^{i+N_w} \underline{x}_{k,f}(i), \quad i = 1, \dots, N_{k,f}. \end{aligned} \quad (9)$$

In order to generate helpful feature representation for fault detection, the linear PCA technology is used as the specific solution to analyze the data in (8). Consider  $X_{nr}$  in (8), the loading matrices in principal and residual subspaces,  $P_p$  and  $P_r$ , could be obtained via the following singular value decomposition:

$$S = [P_p \ P_r] \begin{bmatrix} \Lambda_p & 0 \\ 0 & \Lambda_r \end{bmatrix} [P_p \ P_r]^T \quad (10)$$

where

$$\begin{aligned} S &= \frac{1}{N_{nr} - 1} X_{nr}^T X_{nr} \\ \Lambda_p &= \text{diag}(\lambda_1, \dots, \lambda_l), \quad \text{and} \\ \Lambda_r &= \text{diag}(\lambda_{l+1}, \dots, \lambda_6). \end{aligned} \quad (11)$$

Here,  $l$  is the number of the dimension of the retained principal subspace, which can be determined by the cumulative percent variance method [17]. Different from (1), the mapped feature using PCA method can be obtained by

$$Z_p = X_{nr} P_p \quad \text{and} \quad Z_r = X_{nr} P_r. \quad (12)$$

Similar to (2), all the feature nodes of normal dataset can be defined as

$$Z := [Z_p \ Z_r] \quad (13)$$

where  $Z \in R^{N_{nr} \times 6}$ ,  $Z_p \in R^{N_{nr} \times l}$ , and  $Z_r \in R^{N_{nr} \times (6-l)}$ . Then, the fault detection can be achieved via the following hypothesis test:

$$\begin{aligned} H_0 &: J \leq J_{th} \implies \text{fault-free} \\ H_1 &: \text{otherwise} \implies \text{faulty} \end{aligned} \quad (14)$$

where  $J$  is the test statistic and  $J_{th}$  is its corresponding threshold. In this article,  $J$  for  $Z_p$  and  $Z_r$  can be defined in terms of

$$T_p^2 = \|\Lambda_p^{1/2} Z_p^T\|^2, \quad T_r^2 = \|\Lambda_r^{1/2} Z_r^T\|^2. \quad (15)$$

Accordingly,  $J_{th}$  for  $T^2$  in (15) can be obtained via the probability density functions (pdf) of  $T^2$  and the acceptable significance level  $\alpha$ .

*Remark 1:* The mapped features are obtained via the moving average-PCA, based on which the test statistics are then defined. Main advantages of the aforementioned procedures are as follows.

---

**Algorithm 1:** Off-Line Design for Fault Detection (Inputs:  $X_{nr}$ ; Outputs:  $P_p$ ,  $P_r$ ,  $J_{T_p^2, th}$ , and  $J_{T_r^2, th}$ ).

---

- 1: Preprocess  $X_{nr}$  via the moving average technique and define it as  $X_{nr}$ ;
  - 2: Obtain two loading matrices  $P_p$  and  $P_r$  via (10);
  - 3: Generate the feature nodes via (12) and form the feature matrix  $Z$  via (13);
  - 4: Define two test statistics in terms of (15) and determine their corresponding thresholds  $J_{T_p^2, th}$  and  $J_{T_r^2, th}$  based on PDFs of  $T^2$  and given  $\alpha$ .
- 

- 1) By incorporating historical information hidden in a sliding window, the moving average technique has an improved performance on detecting small abnormalities [17].
- 2) It is of highly computational efficiency because of the powerful ability in processing original data via PCA [36].
- 3)  $T^2$  defined in (15) can deliver optimal detectability for additive faults. [37].

▽

Based on the abovementioned discussion, the fault detection algorithm using mapped features in the offline phase is summarized in the following algorithm.

### C. Fault Diagnosis Using the Broad Model

As mentioned in Section III-A, the data acquisition system equipped in high-speed trains provides sufficient datasets, including both normal and fault datasets. These fault datasets are the fundamentals for successful fault diagnosis for high-speed trains using the broad learning system.

Given  $X_{k,f}$  in (8) for  $k = 1, \dots, K$ , all the feature nodes of  $X_{k,f}$  can be obtained based on the established PCA model as follows:

$$Z_{k,p} = X_{k,f} P_p, \quad Z_{k,r} = X_{k,f} P_r. \quad (16)$$

Then, the  $k$ th feature matrix corresponding to the  $k$ th type of faults can be formed by

$$Z_k := [Z_{k,p} \ Z_{k,r}]. \quad (17)$$

The  $m$  sets of enhancement nodes corresponding to the  $k$ th type of faults can be obtained by the following random projections:

$$H_{k,j} = \varphi_j(Z_k W_{h_j} + \beta_{h_j}^T), \quad j = 1, \dots, m. \quad (18)$$

The enhancement matrix including  $m$  sets of enhancement nodes can be further defined as

$$H^m = [H_{k,1} \ H_{k,2} \ \cdots \ H_{k,m}] \quad (19)$$

where  $H_{k,j} \in R^{N_{k,f} \times q}$  and  $H^m \in R^{N_{k,f} \times mq}$ . Hence, the broad model used for fault diagnosis, according to (5), can be obtained in terms of

$$\begin{aligned} Y_k &= [Z_k | H_{k,1} \ H_{k,2} \ \cdots \ H_{k,m}] W_k^m \\ &= [Z_k | H^m] W_k^m \end{aligned} \quad (20)$$

---

**Algorithm 2:** Off-Line Design for Fault Diagnosis (Inputs:  $\underline{X}_{k,f}$ ; Outputs:  $W$ ).

---

- 1: Define  $Z_k$  via (17) based on the moving average technique and loading matrices (i.e.,  $P_p$  and  $P_r$ ) obtained from Algorithm 1;
  - 2: Set  $j = 1$  and  $j \leq m$ ;
  - 3: Generate random parameters  $W_{h_j}$  and  $\beta_{h_j}$ ;
  - 4: Obtain  $j$ -th enhancement node  $H_{k,j}$  via (18);
  - 5: If  $j < m$ , then  $j = j + 1$  and go back to 3; otherwise, continue;
  - 6: Define the enhancement matrix  $H^m$  via (19);
  - 7: Calculate the weighted matrix  $W^m$  via the ridge regression approximation method;
  - 8: Compute the MR via (22);
  - 9: If MR is acceptable, go to Step 11; otherwise, continue;
  - 10: Generate a set of new random parameters  $W_{h_{m+1}}$  and  $\beta_{h_{m+1}}$ , then compute  $H^{m+1}$  and  $W^{m+1}$ ; and go back to Step 8;
  - 11: Output  $W$ .
- 

where the weighted matrix  $W_k^m$  can be calculated via the ridge regression approximation [34] such that  $W_k^m = [Z_k | H_{k,j}]^\dagger Y \in R^{(6+qm) \times K}$ .

Here,  $Y_k$  is the output of the modified broad model, which corresponds to the  $k$ th type of faults. In this article, the misdiagnosis rate (MR) of  $f_k$  can be defined as follows:

$$\text{MR} = P(f_{\bar{k}} | f_k), \bar{k} \neq k. \quad (21)$$

In order to obtain the optimal parameter  $W^m$ , MR is adopted as the training error of the modified broad model. Hence, (21) can be equivalently calculated by

$$\text{MR} = P(Y_{\bar{k}} | Y_k), \bar{k} \neq k. \quad (22)$$

Compared with the existing fault diagnosis methods using neural networks such as [32], the optimized computational efficiency of our proposed method can be easily achieved, as summarized in the following remark.

*Remark 2:* It is worth pointing out that: 1) the designed FDD method from (16) to (22) can be carried out when the fault-data sampling with the corresponding labels are received; 2) without using deep structures of neural networks, the improved ability of fault diagnosis can be accomplished via broadening the network structure.  $\nabla$

Combing with Algorithm 1, the training using the broad model for fault diagnosis purpose in offline phase can be summarized in Algorithm 2.

As described in Algorithm 2, the update of the BLS is focused on the increment of enhancement nodes to improve the learning ability, and hence, to enhance the performance of fault diagnosis.

*Remark 3:* Without sophisticated design or *a priori* on traction systems of high-speed trains, the essential idea of the proposed method is that the modified PCA has been embedded into BLS to generate real-time decision of FDD.  $\nabla$

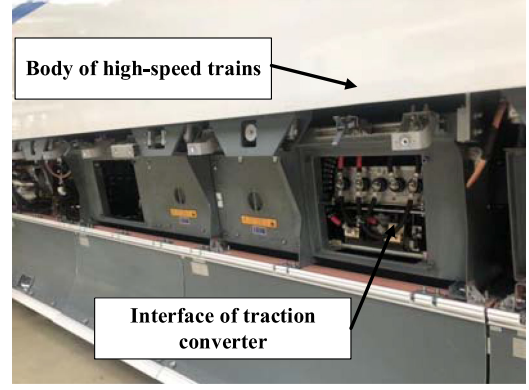


Fig. 4. Traction converters of high-speed trains.

---

**Algorithm 3:** Online Fault Detection and Diagnosis (Input:  $\underline{x}_{on}$ ; Output:  $Y_k$ ).

---

- 1: Read a new observation  $\underline{x}_{on}$  and form  $x_{on}$  in a sliding window according to (9);
  - 2: Recall the training parameters  $P_p, P_r, J_{T_p^2, th}$ , and  $J_{T_r^2, th}$  in Algorithm 1 and  $W$  in Algorithm 2;
  - 3: Declare an alarm if a fault appears according to (12) and (15), and continue; otherwise, go back to step 1;
  - 4: Make a fault decision on  $\underline{x}_{on}$  according to (17), (19), and (20); go back to Step 1.
- 

#### D. Online Implementation of Fault Detection and Diagnosis

Following two training procedures presented in Algorithms 1 and 2, the online implementation of FDD with superior computational efficiency and diagnostic accuracy is formulated in Algorithms 3.

## IV. EXPERIMENTS

In this section, case studies including detection and diagnosis of incipient faults in traction systems platform of a high-speed train [38] will be described in detail. It is used for fault injection online. As a testing system before train operation, this platform has important guiding significance. The testing results are also have a critical reference value for high-speed trains.

#### A. Fault Types of Traction Control System

The experimental model is constructed via dSPACE that contains the motors, transformers, and inverters presented in Figs. 4 and 5. In this application, three typical types of incipient sensor faults are considered as follows.

- 1) *Fault case f1:* The first fault  $f_1$  occurs in the current sensor for A-phase after 400 s. This type of fault has strong transmission characteristics, it will propagate to the whole traction system because of the feedback of the double-PI controller and thereby affects the whole system performance. Here,  $f_1 = 0.15$  A.
- 2) *Fault case f2:* The second fault  $f_2$  is introduced on the upper bridge of dc link after 400 s in an open-loop manner.

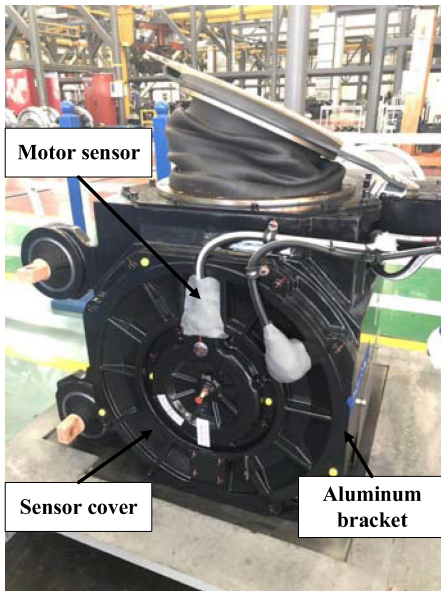


Fig. 5. Traction motors of high-speed trains.

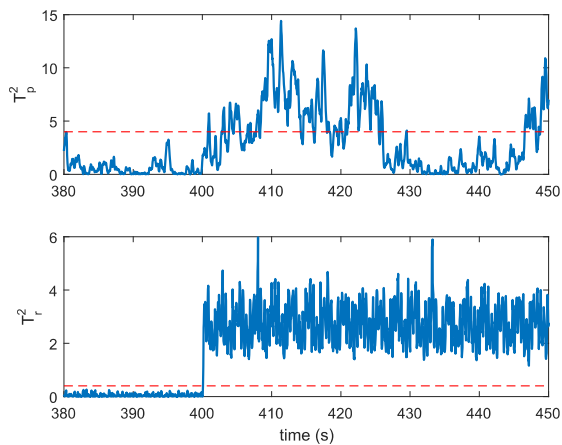


Fig. 6. Detection results for  $f_1$ .

The characteristic is that the injected fault will only affect the monitoring results. Here,  $f_2 = 10$  V.

- 3) *Fault case  $f_3$* : The last fault  $f_3$  arises by incipient changes in the speed sensor after 400 s. The characteristics are similar to those of  $f_1$ , this fault will affect the performance of the traction system because of the feedback controller.

It should be noted that the abovementioned incipient faults were suggested by engineers of high-speed trains such that they are usually considered in the practical high-speed trains.

### B. Fault Detection and Diagnosis

Detailed detection results adopting the proposed method for incipient faults abovementioned are given in Figs. 6 through 8 where blue solid lines are test statistics defined in (15) and red dotted lines are the corresponding thresholds. The confusion matrix, which is also called as an error matrix, can display fault diagnosis results. In accordance with (21) and (22), a confusion

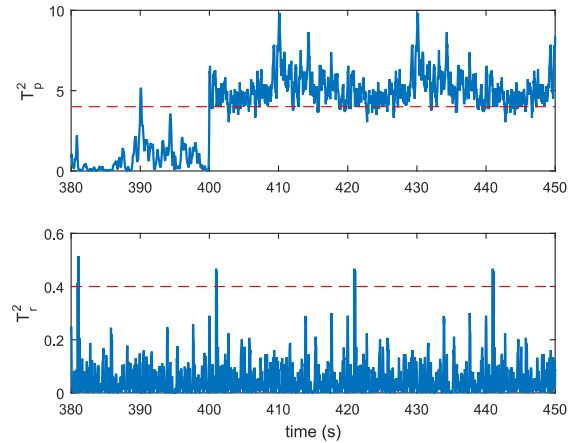


Fig. 7. Detection results for  $f_2$ .

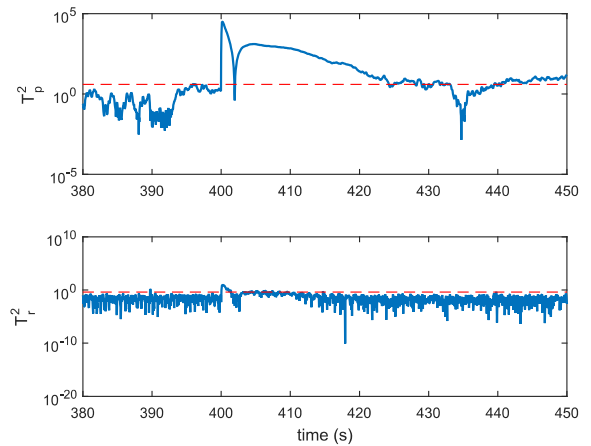


Fig. 8. Detection results for  $f_3$ .

matrix corresponds to a ratio, the analysis of which shows that fault should be  $k$ th one, but it turns out to be  $\bar{k}$ th fault, where  $k = 1, 2, 3$ . After successful detection of faults, the diagnosis results using Algorithm 3 are summarized via the confusion matrix in Fig. 9.

Fig. 6 presents the detection results for  $f_1$  using mapped features in the proposed method. It can be easily observed that  $T_p^2$  can promptly declare this fault while  $T_r^2$  fluctuates up and down across its threshold because of the effective double-PI controller [39]. The detection results can not only show the effectiveness of the designed algorithm to detect  $f_1$  but also are consistent with the description on this fault.

Based on the depiction in Fig. 7, the proposed method can rapidly detect  $f_2$  by  $T_p^2$  after its occurrence. Whilst,  $T_r^2$  is not sensitive to  $f_2$ , it does not have obvious fluctuations caused by the regulating effect of the double-PI controller. In addition, there is a false alarm in 390 s. Actually, false alarms are permissible within a reasonable range. It is clear from Fig. 7 that the fault can be detected successfully.

After  $f_3$  is introduced to the speed sensor, great fluctuations caused by the regulating effect of the double-PI controller appear after 400 s, as displayed in Fig. 8. However, before  $T_r^2$  returns to

$f_1$	1894 31.7%	0 0.0%	37 0.6%	98.1% 1.9%
$f_2$	1 0.0%	2024 33.9%	1 0.0%	99.9% 0.1%
$f_3$	90 1.5%	0 0.0%	1924 32.2%	95.5% 4.5%
	95.4% 4.6%	100% 0.0%	98.1% 1.9%	97.8% 2.2%
	$f_1$	$f_2$	$f_3$	

Fig. 9. Confusion matrix of diagnostic results for three faults using the proposed method.

$f_1$	216 4.8%	80 1.8%	121 2.7%	1 0.0%	51.7% 48.3%
$f_2$	391 8.7%	861 19.1%	71 1.6%	1 0.0%	65.0% 35.0%
$f_3$	380 8.4%	46 1.0%	823 18.3%	2 0.0%	65.8% 34.2%
normal	0 0.0%	0 0.0%	0 0.0%	1506 33.5%	100% 0.0%
	21.9% 78.1%	87.2% 12.8%	81.1% 18.9%	99.7% 0.3%	75.7% 24.3%
	$f_1$	$f_2$	$f_3$	normal	

Fig. 10. Confusion matrix of diagnostic results for four conditions using BLS.

 TABLE I  
 PERFORMANCE COMPARISON USING SIX METHODS

Method	Diagnostic accuracy	Total training time	Average test time for per sample
1D-CNN (four conditions)	85.2%	121.2s	$20.2 \times 10^{-3}$ s
LSTM (four conditions)	55.7%	235.3s	$51.3 \times 10^{-3}$ s
BLS (three conditions)	76.3%	15.17s	$0.17 \times 10^{-3}$ s
BLS (four conditions)	75.7%	14.16s	$0.17 \times 10^{-3}$ s
PCA+BLS (four conditions)	88.3%	23.65s	$0.18 \times 10^{-3}$ s
The proposed method (four conditions)	97.8%	22.9s	$0.18 \times 10^{-3}$ s

the normal level, it only shows partial and unsatisfactory detection performance. Fortunately, although  $T_p^2$  cannot successfully detect  $f_3$  from 433 s and 438 s, its fault-detecting capability has recovered after 438 s.

Based on the abovementioned detection results, fast diagnosis has been achieved. The results of fault diagnosis are summarized in Fig. 9. The diagnostic accuracy for  $f_2$  and  $f_3$  is higher than that for  $f_1$ . In general, the total diagnostic accuracy for three incipient faults is 97.8% and, thus, is satisfactory in practice.

### C. Discussions

In order to demonstrate the superior performance of the proposed method including diagnostic accuracy and computational accuracy, comparison results using six methods are given in Table I. The diagnostic performance of deep learning and broad learning was compared under different conditions. In this study, a favorable setting is used for obtaining the reliable results. In addition, as shown in Table I, four conditions mean that the training and test datasets cover the operation conditions under normal,  $f_1$ ,  $f_2$ , and  $f_3$ ; three conditions only consider the operations with  $f_1$ ,  $f_2$ , and  $f_3$ .

It is easy to see that, based on diagnostic results in Table I, improvements of the proposed method over other five methods

$f_1$	1727 22.3%	0 0.0%	32 0.4%	349 4.5%	81.9% 18.1%
$f_2$	0 0.0%	1931 24.9%	0 0.0%	2 0.0%	99.9% 0.1%
$f_3$	35 0.5%	0 0.0%	1913 24.7%	171 2.2%	90.3% 9.7%
normal	205 2.6%	0 0.0%	112 1.4%	1264 16.3%	79.9% 20.1%
	87.8% 12.2%	100% 0.0%	93.0% 7.0%	70.8% 29.2%	88.3% 11.7%
	$f_1$	$f_2$	$f_3$	normal	

Fig. 11. Confusion matrix of diagnostic results for four conditions using PCA and BLS.

for FDD are indicated explicitly. Meanwhile, the test time for per sample is  $1.8 \times 10^{-4}$ s, which is less than the sampling interval  $4 \times 10^{-4}$ s [17]. It should be noted that the proposed method in this article is different from ‘‘PCA+BLS’’, which is adopted the original method in both fault detection and diagnosis.

In addition, the diagnostic results directly using BLS are shown in Fig. 10. Although the BLS can make faster fault decision than our proposed method, its diagnostic accuracy is only 75.7%, which will cause a number of false alarms. Similar to the direct applications using BLS, PCA, and BLS can be also used to make a direct fault decision for four conditions, and the corresponding results are given in Fig. 11. It can be clearly observed that, the total diagnostic accuracy of this method is 88.3%, which is unsatisfactory. Meanwhile, the direct use of PCA and BLS can cause more computational loads than the proposed method because more parameters need to be trained and obtained. The FDD framework proposed in this article has achieved a satisfactory diagnostic result. But there are still some problems for applications.

- 1) The distribution of data is non-Gaussian, which increases the difficulty of feature extraction in traction systems.

- 2) The characteristics of high sampling frequency, large-scale measurement points, and multisource data bring challenges to FDD task.
- 3) Massive amounts of data lead to heavy computing loads. The demand of real-time ability for traction systems is an urgent problem.

## V. CONCLUSION

In this article, a real-time and data-driven fault diagnosis scheme for traction systems of high-speed trains has been investigated. An enhanced fault detection and diagnosis architecture using the modified principal component analysis and broad learning system has been developed in this article. The experiments on traction systems have clearly demonstrated that the proposed FDD method can effectively reduce the computational load while maintaining the satisfactory diagnostic accuracy. Based on this study, future challenging issues will be focused on performance evaluation and fault prognosis using MSA and BLS techniques.

## REFERENCES

- [1] H. Chen, B. Jiang, N. Lu, and W. Chen, *Data-Driven Detection and Diagnosis of Faults in Traction Systems of High-Speed Trains*. New York, NY, USA: Springer, 2020.
- [2] C. Yang *et al.*, "Voltage difference residual-based open-circuit fault diagnosis approach for three-level converters in electric traction systems," *IEEE Trans. Power Electron.*, vol. 35, no. 3, pp. 3012–3028, Mar. 2020.
- [3] D. Zhou, H. Qiu, S. Yang, and Y. Tang, "Submodule voltage similarity-based open-circuit fault diagnosis for modular multilevel converters," *IEEE Trans. Power Electron.*, vol. 34, no. 8, pp. 8008–8016, Aug. 2019.
- [4] Z. Chen and K. E. Haynes, *Chinese Railways in the Era of High-speed*. Bingley, U.K.: Emerald Group, 2015.
- [5] D. Ronanki, S. A. Singh, and S. S. Williamson, "Comprehensive topological overview of rolling stock architectures and recent trends in electric railway traction systems," *IEEE Trans. Transport. Electric.*, vol. 3, no. 3, pp. 724–738, Sep. 2017.
- [6] M. Givoni, "Development and impact of the modern high-speed train: A review," *Transp. Rev.*, vol. 26, no. 5, pp. 593–611, Feb. 2006.
- [7] P. H. Bowers, "Railway reform in Germany," *J. Transp. Econ. Policy*, vol. 30, no. 1, pp. 95–102, Jan. 1996.
- [8] S. Zhang, *Fundamental Application Theory and Engineering Technology for Railway High-speed Trains*. Beijing, China: Science Press, 2007.
- [9] D. Feng, S. Lin, Q. Yang, X. Lin, Z. He, and W. Li, "Reliability evaluation for traction power supply system of high-speed railway considering relay protection," *IEEE Trans. Transport. Electric.*, vol. 5, no. 1, pp. 285–298, Mar. 2019.
- [10] H. Chen and B. Jiang, "A review of fault detection and diagnosis for the traction system in high-speed trains," *IEEE Trans. Intell. Transp. Syst.*, vol. 21, no. 2, pp. 450–465, Feb. 2020.
- [11] J. Wang, J. Wang, C. Roberts, and L. Chen, "Parallel monitoring for the next generation of train control systems," *IEEE Trans. Intell. Transp. Syst.*, vol. 16, no. 1, pp. 330–338, Feb. 2015.
- [12] Z. Xu, W. Wang, and Y. Sun, "Performance degradation monitoring for onboard speed sensors of trains," *IEEE Trans. Intell. Transp. Syst.*, vol. 13, no. 3, pp. 1287–1297, Sep. 2012.
- [13] H. Chen, B. Jiang, N. Lu, and Z. Mao, "Deep PCA based real-time incipient fault detection and diagnosis methodology for electrical drive in high-speed trains," *IEEE Trans. Veh. Technol.*, vol. 67, no. 6, pp. 4819–4830, Jun. 2018.
- [14] A. Romanenko, A. Muetze, and J. Ahola, "Incipient bearing damage monitoring of 940-h variable speed drive system operation," *IEEE Trans. Energy Convers.*, vol. 32, no. 1, pp. 99–110, Mar. 2017.
- [15] K. Hu *et al.*, "Cost-effective prognostics of IGBT bond wires with consideration of temperature swing," *IEEE Trans. Power Electron.*, vol. 35, no. 7, pp. 6773–6784, Jul. 2020.
- [16] D. Zhou, H. Ji, X. He, and J. Shang, "Fault detection and isolation of the brake cylinder system for electric multiple units," *IEEE Trans. Control Syst. Technol.*, vol. 26, no. 5, pp. 1744–1757, Sep. 2018.
- [17] H. Chen, B. Jiang, W. Chen, and H. Yi, "Data-driven detection and diagnosis of incipient faults in electrical drives of high-speed trains," *IEEE Trans. Ind. Electron.*, vol. 66, no. 6, pp. 4716–4725, Jun. 2019.
- [18] D. Zhou and Y. Tang, "A model predictive control-based open-circuit fault diagnosis and tolerant scheme of three-phase AC-DC rectifiers," *IEEE J. Emerg. Sel. Topics Power Electron.*, vol. 7, no. 4, pp. 2158–2169, Dec. 2019.
- [19] J. Wang, H. Wu, T. Yang, L. Zhang, and Y. Xing, "Bidirectional three-phase dc-ac converter with embedded dc-dc converter and carrier-based PWM strategy for wide voltage range applications," *IEEE Trans. Ind. Electron.*, vol. 66, no. 6, pp. 4144–4155, Jun. 2019.
- [20] C. Cheng, J. Wang, Z. Zhou, W. Teng, Z. Sun, and B. Zhang, "A BRB-based effective fault diagnosis model for high-speed trains running gear systems," *IEEE Trans. Intell. Transp. Syst.*, to be published, doi:10.1109/TITS.2020.3008266.
- [21] K. Wang, E. Tian, J. Liu, L. Wei, and D. Yue, "Resilient control of networked control systems under deception attacks: A memory-event-triggered communication scheme," *Int. J. Robust Nonlinear Control*, vol. 30, no. 4, pp. 1534–1548, Mar. 2020.
- [22] S. X. Ding, *Model-Based Fault Diagnosis Techniques: Design Schemes, Algorithms, and Tools*. Berlin, Germany: Springer Science & Business Media, 2008.
- [23] R. Isermann, "Model-based fault-detection and diagnosis—status and applications," *Ann. Rev. Control*, vol. 29, no. 1, pp. 71–85, Jan. 2005.
- [24] D. Barater, J. Arellano-Padilla, and C. Gerada, "Incipient fault diagnosis in ultrareliable electrical machines," *IEEE Trans. Ind. Appl.*, vol. 53, no. 3, pp. 2906–2914, May 2017.
- [25] X. He, Z. Wang, Y. Liu, and D. Zhou, "Least-squares fault detection and diagnosis for networked sensing systems using a direct state estimation approach," *IEEE Trans. Ind. Inform.*, vol. 9, no. 3, pp. 1670–1679, Aug. 2013.
- [26] H. Chen, B. Jiang, and N. Lu, "A newly robust fault detection and diagnosis method for high-speed trains," *IEEE Trans. Intell. Transp. Syst.*, vol. 20, no. 6, pp. 2198–2208, Jun. 2019.
- [27] J. Wang, Y. Xing, H. Wu, and T. Yang, "A novel dual-dc-port dynamic voltage restorer with reduced-rating integrated dc-dc converter for wide-range voltage sag compensation," *IEEE Trans. Power Electron.*, vol. 34, no. 8, pp. 7437–7449, Aug. 2019.
- [28] Z. Chen *et al.*, "A just-in-time-learning aided canonical correlation analysis method for multimode process monitoring and fault detection," *IEEE Trans. Ind. Electron.*, to be published, doi: 10.1109/TIE.2020.2989708.
- [29] Z. Chen, S. X. Ding, T. Peng, C. Yang, and W. Gui, "Fault detection for non-gaussian processes using generalized canonical correlation analysis and randomized algorithms," *IEEE Trans. Ind. Electron.*, vol. 65, no. 2, pp. 1559–1567, Feb. 2018.
- [30] A. Giantomassi, F. Ferracuti, S. Iarlori, G. Ippoliti, and S. Longhi, "Electric motor fault detection and diagnosis by kernel density estimation and kullback-leibler divergence based on stator current measurements," *IEEE Trans. Ind. Electron.*, vol. 62, no. 3, pp. 1770–1780, Mar. 2015.
- [31] W. He, Y. He, and C. Zhang, "A new fault diagnosis approach for analog circuits based on spectrum image and feature weighted kernel Fisher discriminant analysis," *Rev. Sci. Instrum.*, vol. 89, no. 7, Jun. 2018, Art. no. 074702.
- [32] K. Watanabe, I. Matsuura, M. Abe, M. Kubota, and D. M. Himmelblau, "Incipient fault diagnosis of chemical processes via artificial neural networks," *AIChE J.*, vol. 35, no. 11, pp. 1803–1812, Nov. 1989.
- [33] J. Feng, J. Xu, W. Liao, and Y. Liu, "Review on the traction system sensor technology of a rail transit train," *Sensors*, vol. 17, no. 6, pp. 1–16, Jun. 2017.
- [34] C. L. P. Chen and Z. Liu, "Broad learning system: An effective and efficient incremental learning system without the need for deep architecture," *IEEE Trans. Neural Netw. Learn. Syst.*, vol. 29, no. 1, pp. 10–24, Jan. 2018.
- [35] Z. Liu, J. Zhou, and C. L. P. Chen, "Broad learning system: Feature extraction based on k-means clustering algorithm," in *Proc. 4th Inf. Cybern. Comput. Social Syst. Conf.*, Dalian, 2017, pp. 683–687.
- [36] S. J. Qin, "Survey on data-driven industrial process monitoring and diagnosis," *Ann. Rev. Control*, vol. 36, no. 2, pp. 220–234, Dec. 2012.
- [37] S. X. Ding, *Data-driven Design of Fault Diagnosis and Fault-tolerant Control Systems*. New York, NY, USA: Springer-Verlag, 2014.
- [38] X. Yang, C. Yang, T. Peng, Z. Chen, B. Liu, and W. Gui, "Hardware-in-the-loop fault injection for traction control system," *IEEE J. Emerg. Sel. Topics Power Electron.*, vol. 6, no. 2, pp. 696–706, Jun. 2018.
- [39] J. W. Finch and D. Giaouris, "Controlled AC electrical drives," *IEEE Trans. Ind. Electron.*, vol. 55, no. 2, pp. 481–491, Feb. 2008.



**Chao Cheng** (Member, IEEE) received the M.Eng. and Ph.D. degrees from Jilin University, Changchun, China, in 2011 and 2014, respectively.

He is currently an Associated Professor with the Changchun University of Technology, Changchun. He has been a Postdoctoral Fellow in process control engineering with the Department of Automation, Tsinghua University, Beijing, China, since 2018. He has also been a Postdoctoral Fellow with the National Engineering Laboratory, CRRC Changchun Railway Vehicles Co., Ltd., China, since 2018. His research interests include dynamic system fault diagnosis and predictive maintenance, wireless sensor network, artificial intelligence, and data-driven method.



**Bangcheng Zhang** received the B.Eng. and M.Eng. degrees from the Changchun University of Technology, Changchun, China, in 1995 and 2004, respectively, and the Ph.D. degree from Jilin University, Changchun, China, in 2011.

He is currently a Professor with the Changchun University of Technology. He has been an Academic Visitor with Tsinghua University, Beijing, China, since 2007. He has authored and coauthored more than 20 articles. His research interests include mechatronics measurement technique and fault diagnosis.



**Weijun Wang** received the B.Eng. degree in 2018 from Changchun University of Technology, Changchun, China, where he is currently working toward the M.Eng. degree in computer science and engineering.

His main research interests include state estimation, distributed sensor network, and fault diagnosis.



**Junjie Shao** received the B.E. degree in computer science and technology from Changchun Normal University Changchun, China, in 2011.

He is currently the Director of the Data Research Office for the CRRC Changchun Railway Vehicles Co., Ltd. He took the lead in building the company's data research platform and continued to carry out basic technology research and engineering promotion for application. The research results in its field have reached an industry-leading level. As a leader, he constructed the company's PHM system, and through

continuous optimization of the PHM system, he provided strong support for the company's market bidding, product design, artificial intelligence for IT operations, and vehicle repairs.



**Hongtian Chen** (Member, IEEE) received the B.S. and M.S. degrees from the School of Electrical and Automation Engineering, Nanjing Normal University, Nanjing, China, in 2012 and 2015, respectively, and the Ph.D. degree from the College of Automation Engineering, Nanjing University of Aeronautics and Astronautics, Nanjing, China, in 2019.

He has been a Visiting Scholar with the Institute for Automatic Control and Complex Systems, University of Duisburg-Essen, Germany, since 2018. He is currently a Postdoctoral Fellow with the Department of

Chemical and Materials Engineering, University of Alberta, Canada. His research interests include process monitoring and fault diagnosis, data mining and analytics, machine learning, and quantum computation; and their applications in high-speed trains, new energy systems, and industrial processes.

Dr. Chen was a recipient of the Grand Prize of Innovation Award of Ministry of Industry and Information Technology of the People's Republic of China in 2019, the Excellent Ph.D. Thesis Award of Jiangsu Province in 2020, and the Excellent Doctoral Dissertation Award from Chinese Association of Automation in 2020.



**Wanxiu Teng** received the B.Eng. and M.Eng. degrees in 2002 and 2010, respectively, from Southwest Jiaotong University, Chengdu, China, where he is currently working toward the Ph.D. degree in mechanical engineering.

He has been a Party Branch Secretary and the Deputy Director of the National Engineering Laboratory, CRRC Changchun Railway Vehicles Co., Ltd., China, since 2015. His research interests include mechatronics measurement technique and fault diagnosis.